

Appearance and disappearance of the mRNA signature characteristic of T_{reg} cells in visceral adipose tissue: Age, diet, and PPAR γ effects

Daniela Cipolletta^{a,1}, Paul Cohen^b, Bruce M. Spiegelman^b, Christophe Benoist^{a,c}, and Diane Mathis^{a,c,2}

^aDivision of Immunology, Department of Microbiology and Immunobiology, Harvard Medical School, Boston, MA 02115; ^bDana-Farber Cancer Institute and Department of Cell Biology, Harvard Medical School, Boston, MA 02215; and ^cEvergrande Center for Immunologic Diseases, Harvard Medical School and Brigham and Women's Hospital, Boston, MA 02115

Contributed by Diane Mathis, December 8, 2014 (sent for review November 25, 2014)

A unique population of Foxp3⁺CD4⁺ regulatory T (T_{reg}) cells resides in visceral adipose tissue (VAT) of lean mice, especially in the epididymal fat depot. VAT T_{regs} are unusual in their very high representation within the CD4⁺ T-cell compartment, their transcriptome, and their repertoire of antigen-specific T-cell receptors. They are important regulators of local and systemic inflammation and metabolism. The overall goal of this study was to learn how the VAT T_{reg} transcriptome adapts to different stimuli; in particular, its response to aging in lean mice, to metabolic perturbations associated with obesity, and to certain signaling events routed through PPAR γ , the "master-regulator" of adipocyte differentiation. We show that the VAT T_{reg} signature is imposed early in life, well before age-dependent expansion of the adipose-tissue T_{reg} population. VAT T_{regs} in obese mice lose the signature typical of lean individuals but gain an additional set of over- and underrepresented transcripts. This obese mouse VAT T_{reg} signature depends on phosphorylation of the serine residue at position 273 of PPAR γ , in striking parallel to a pathway recently elucidated in adipocytes. These findings are important to consider in designing drugs to target type 2 diabetes and other features of the "metabolic syndrome."

obesity | inflammation | type 2 diabetes | regulatory T cell | Foxp3

Inflammation is a major link between obesity and type 2 diabetes (T2D) (1–3). Energy intake in excess of expenditure induces chronic inflammation of visceral adipose tissue (VAT), which eventually provokes inflammation at distant sites and, thereby, metabolic abnormalities such as insulin resistance and dyslipidemia, culminating in T2D and cardiovascular disease. At the core of this "metabolic syndrome" is VAT: Through the production of a variety of adipokines and other mediators, adipocytes in visceral fat depots can positively or negatively influence insulin sensitivity, lipid levels and appetite. Although innate immunocytes, notably macrophages (MFs), have historically been considered to be the drivers of adipose-tissue inflammation and metabolic dysregulation, several recent reports argued for an important effector or regulatory role for adaptive immunocytes, i.e., T, B, or NKT cells.

In particular, a unique population of Foxp3⁺CD4⁺ regulatory T (T_{reg}) cells accumulates in VAT of lean mice as they age (4, 5). Vis-à-vis their lymphoid-tissue counterparts, VAT T_{regs} are remarkable by several criteria. They are highly overrepresented in lean individuals (40–80% vs. 5–15% of the CD4⁺ T-cell compartment). Their transcriptome is distinct, especially the profile of transcripts encoding transcription factors, chemokines/chemokine-receptors, and cytokines/cytokine-receptors, as well as atypical expression of a set of transcripts specifying molecules involved in lipid metabolism. Thirdly, they have an unusual, clonally expanded, repertoire of T-cell antigen receptors (4).

It came as a surprise that PPAR γ , the "master regulator" of adipocyte differentiation (6), is also a crucial molecular orchestrator of VAT T_{reg} cell accumulation, phenotype and function (5). T_{reg}-specific ablation of *Pparg* greatly reduced the VAT T_{reg} population, while not affecting lymphoid-tissue T_{regs}, in mice

maintained on a normal-chow diet (NCD). Conversely, injection of the PPAR γ agonist, pioglitazone (pio), into mice kept on a high-fat diet (HFD) expanded the T_{reg} population in VAT but not lymphoid tissues. Cotransduction experiments revealed that PPAR γ worked together with Foxp3 to impose the unique transcriptome of VAT T_{regs}; the sets of genes over- or underrepresented in CD4⁺ T cells transduced with *Foxp3* plus *Pparg* in comparison with *Foxp3* alone was enriched for the previously defined VAT T_{reg} up- and down-signatures.

The overall goal of the set of experiments reported herein was to further elucidate the VAT T_{reg} signature: its appearance in lean mice as they age; disappearance in obese mice; and its response to PPAR γ -mediated signaling events. Our data document a number of age- and diet-dependent influences on the VAT T_{reg} transcriptome, and reveal that, as in adipocytes, the effect of obesity on transcription in VAT T_{regs} does not reflect a reduction in their expression of the *Pparg* gene, but rather a posttranslational modification of PPAR γ proteins.

Results

Appearance of the VAT T_{reg} Signature in Lean Mice as they Age. Our first goal was to learn how the transcriptome of VAT T_{regs} evolves over time in lean mice, given that insulin resistance is an age-dependent process. The epididymal fat depot was removed from cohorts of male C57BL/6 (B6) mice at increasing ages, and

Significance

A unique population of Foxp3⁺CD4⁺ regulatory T (T_{reg}) cells resides in visceral adipose tissue of lean mice. VAT T_{regs} are important regulators of local and systemic inflammation and metabolism. Here, we show that the VAT T_{reg} signature is imposed early in life, well before the typical age-dependent expansion of the adipose-tissue T_{reg} population. VAT T_{regs} in obese mice lose the signature typical of lean individuals but gain an additional set of over- and underrepresented transcripts. In striking parallel to a pathway recently elucidated in adipocytes, the obese mouse VAT T_{reg} signature depends on phosphorylation of a specific residue of PPAR γ . These findings are important to consider in designing drugs to target type 2 diabetes and other features of the "metabolic syndrome."

Author contributions: D.C. and D.M. designed research; D.C. performed research; P.C. and B.M.S. contributed new reagents/analytic tools; D.C. and C.B. analyzed data; and D.C., P.C., B.M.S., and D.M. wrote the paper.

The authors declare no conflict of interest.

Data deposition: The data reported in this paper have been deposited in the Gene Expression Omnibus (GEO) database, www.ncbi.nlm.nih.gov/geo (accession no. GSE37535).

¹Present address: Clinical Translational Oncology, Novartis Institute for Biomedical Research, Cambridge, MA 02139.

²To whom correspondence should be addressed. Email: cbdm@hms.harvard.edu.

This article contains supporting information online at www.pnas.org/lookup/suppl/doi:10.1073/pnas.1423486112/-DCSupplemental.

was digested with collagenase to separate floating mature adipocytes from the other cells, referred to as the stromal vascular fraction (SVF). Foxp3⁺CD4⁺ T_{regs} within the SVF were enumerated and further characterized by flow cytometry. Control splenic and/or lymph node (LN) T_{regs} from the same individuals were assessed in parallel. At 5 wk of age, the fraction of T_{regs} in the VAT CD4⁺ T-cell compartment was similar to, even a bit lower than, that typical of lymphoid organs (Fig. 1A). The fraction in VAT gradually rose at 14 and 25 wk of age, and then descended quite precipitously at 40 wk (Fig. 1A), accompanied by a decline in insulin sensitivity (Fig. S1). Meanwhile, the percentage of splenic T_{regs} remained stable at 15–20% (Fig. 1A). A similar rise and fall of the VAT, but not splenic, T_{reg} population was evident when their number, rather than fractional representation, was quantified (Fig. 1B).

We previously reported that the transcription factor, Gata3, is a useful marker for bona fide VAT T_{regs} [given the absence of an appropriate monoclonal antibody (mAb) for cytofluorimetric detection of PPARγ] (5). The fraction of Gata3⁺ T_{regs} in VAT also rose at 14 and 24 wk of age and fell at 40 wk, whereas the fraction in the spleen was constantly low (Fig. 1C).

To follow corresponding evolution of the VAT transcriptome, we performed microarray-based gene-expression profiling of Foxp3⁺CD4⁺ T cells from the LNs vs. the SVF of VAT from B6 mice at increasing ages. Although the transcriptional profiles of VAT and LN T_{regs} were already distinct at 5 wk of age, the total number of loci differentially expressed ≥twofold in VAT mounted at 14 wk and peaked at 25 wk of age (Fig. 2A). This

increase reflected evolution of the VAT T_{reg} transcriptome as there were very few differences in the gene-expression profiles of LN T_{regs} from 5- and 25-wk-old mice (Fig. 2B). Analogous to the numerical decline in Tregs at 40 wk of age, the VAT:LN T_{reg} gene-expression differential also dropped at this age (Fig. 2A).

Using microarray data from 25-wk-old lean mice, we generated “VAT T_{reg}” signatures, comprised of 437 genes up-regulated and 71 genes down-regulated ≥twofold in VAT T_{regs} vs. VAT conventional T (T_{conv}) cells, LN T_{regs} and LN T_{conv} cells (Dataset S1; see its legend for details of signature generation). This signature is more robust than the one previously reported (4) because the various T-cell populations were double-sorted to extremely high purity and because the newer microarray platform encompasses a higher fraction of the genome. Superimposing the VAT T_{reg} signature on the VAT vs. LN T_{reg} comparison plots revealed that the bulk of the signature genes were divergently expressed (i.e., displaced from the diagonal) already at 5 wk of age—notably, paradigmatic VAT transcripts such as *Pparg*, *Gata3*, *Klhl1*, *Ccr2*, and *Il1rl1* (Fig. 2C). Nonetheless, the differential gradually increased to 24 wk, but shrank noticeably at 40 wk of age (Fig. 2C). This age-dependent evolution of the VAT Treg signature, and its persistent distinction from the LN gene-expression profile, is readily apparent from the principal components analysis illustrated in Fig. 2D.

Disappearance of the VAT T_{reg} Signature in Obese Mice. Next, we addressed how the transcriptome of VAT T_{regs} responds to metabolic dysregulation. Two insulin-resistant mouse models of obesity

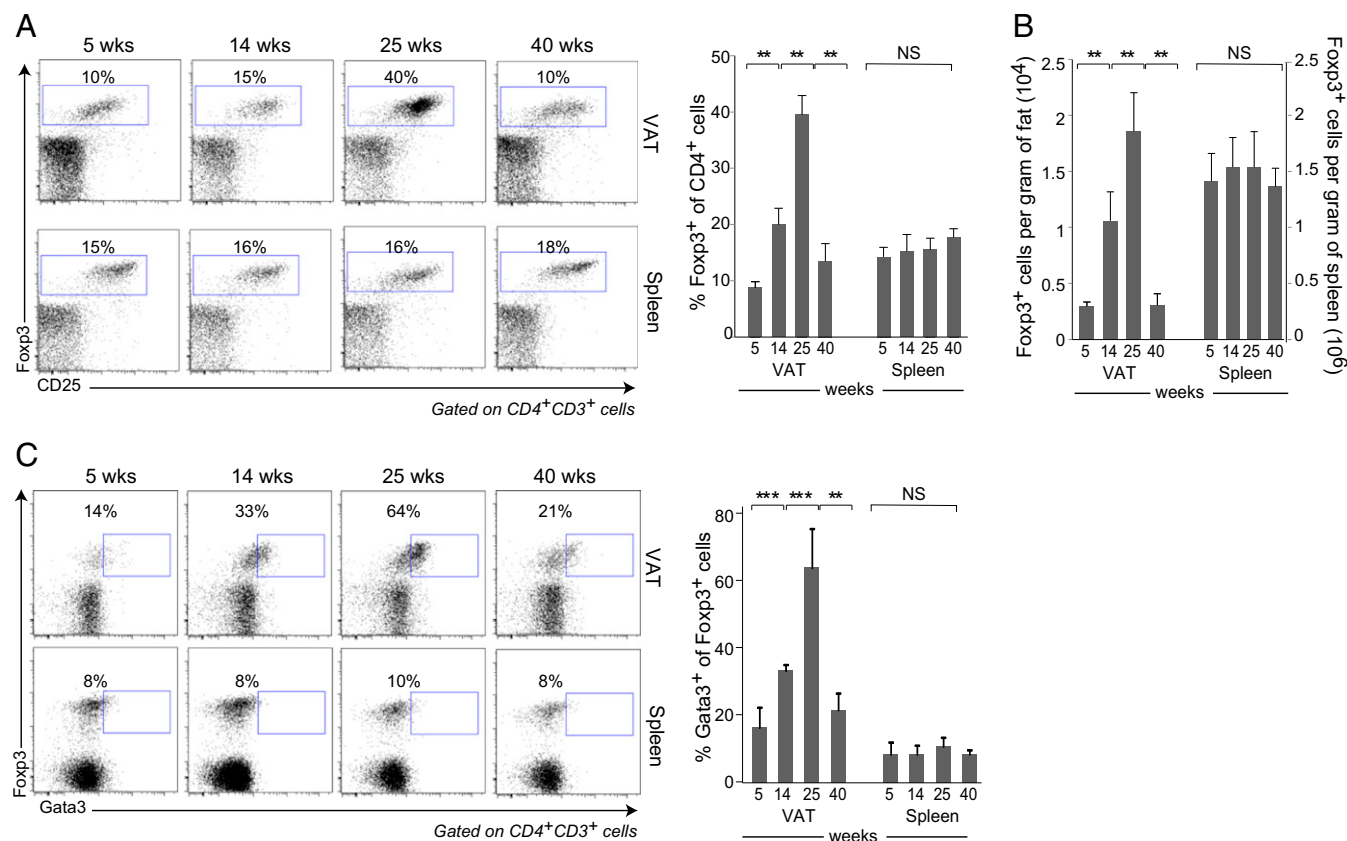


Fig. 1. T_{reg} dynamics and phenotype with aging. T_{regs} were isolated from VAT and spleen of lean B6 males at the indicated ages. (A) Cytofluorimetric analysis of Foxp3⁺CD4⁺CD3⁺ T cells. (Left) Representative dot plots. Numbers indicate the percentage Foxp3⁺ of CD4⁺ cells for that particular experiment. (Right) Summary data from at least three independent experiments. (B) T_{reg} numbers for the same mice. (C) As per A, except Gata3⁺Foxp3⁺ cells were examined. Numbers refer to the percentage Gata3⁺ of Foxp3⁺ cells for that particular experiment. Mean ± SD; ***P* < 0.01; ****P* < 0.001; NS, not significant; by the Student's *t* test.

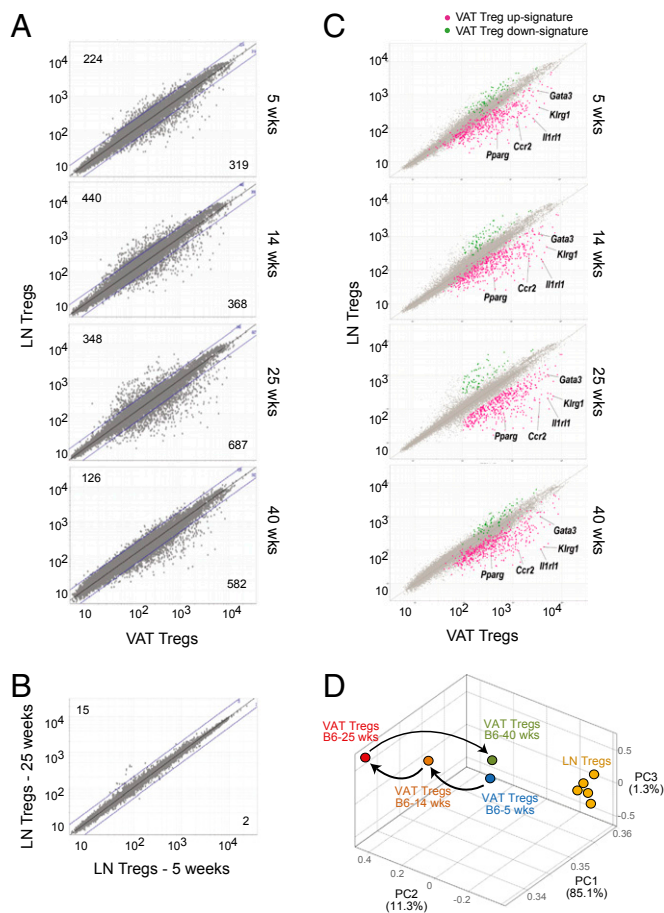


Fig. 2. T_{reg} transcriptome evolution with aging. (A) Normalized microarray-determined expression values for transcripts from VAT vs. LN T_{regs} of B6 mice. Values in the corners refer to numbers of transcripts up- (Upper) or down- (Lower) regulated in VAT T_{regs}. Lines indicate the twofold cutoff. (B) As in panel A except LN transcriptomes from 5- and 25-wk-old mice are compared. (C) Same data as in A except the VAT Treg up- (pink) and down- (green) signatures are overlain (from Dataset S1). (D) Principal components analysis of the same microarray data.

were compared with their lean counterparts: 14-wk-old leptin-deficient (B6.Lep^{ob/ob}; hereafter referred to as B6-ob/ob) mice versus B6 wild-type (B6-WT) littermates; and B6 animals maintained on HFD versus NCD between 8 and 16 wk of age. As previously reported (4), both genetically promoted and diet-induced obesity resulted in a clear reduction in the T_{reg} fraction and number in VAT, while not in the spleen (Fig. 3A and B). In addition, a lower proportion of VAT, but not splenic, T_{regs} expressed detectable levels of Gata3 in the two obese models (Fig. 3C). Under the conditions we chose, the VAT T_{reg} changes were more pronounced in the B6-ob/ob than the HFD model, not surprising given that the former were distinctly more obese (6 g heavier on average).

In both obese models, the T_{regs} that persisted in the adipose tissue were no longer bona fide VAT T_{regs}. This finding is perhaps most evident from the Fold-Change (FC) versus *P* value volcano plots of Fig. 3D, which show a significant underrepresentation of the VAT T_{reg} up-signature and overrepresentation of the corresponding down-signature. Dampening of the characteristic VAT T_{reg} gene-expression profile could reflect alterations at the molecular level (i.e., genes turned up or down), the cellular level (e.g., VAT T_{regs} replaced by lymphoid-tissue T_{regs}) or a mixture of the two. The fact that the transcript “cross-overs” were never complete, some elements of the up-signature remaining overexpressed

and some members of the down-signature still underexpressed in VAT T_{regs} of obese mice, argues that the transcriptome changes do not simply reflect replacement of VAT by lymphoid-tissue T_{regs}. We were able to confirm transcript changes at the protein level via cytofluorimetric analysis of gated T_{regs} (Fig. 3E).

To generate a transcriptional signature for the VAT T_{reg} characteristic of obese mice (which will be referred to as the omVAT T_{reg} signature), we combined the sets of transcripts differentially expressed ≥ 1.5 -fold in either of the two models (Fig. 3F and Dataset S2). The substantially larger number of overrepresented transcripts in the genetically promoted than in the diet-induced obesity model may reflect leptin-dependent transcriptional effects or may simply result from the more advanced obesity in B6-ob/ob mice. Pathway analysis using the Ingenuity and DAVID programs highlighted lymphocyte activation ($P = 10^{-7}$), cytokine/cytokine-receptor ($P = 10^{-4}$) and chemokine/chemokine receptor ($P = 10^{-3}$) pathways in the omVAT T_{reg} up-signature. Sterol (10^{-7}) and steroid (10^{-6}) biosynthesis pathways emerged from pathway analysis of the corresponding down-signature.

Phosphorylation of PPAR γ in Cultured VAT T_{reg} Recapitulates the Transcriptome Changes Provoked by Obesity in Vivo. Interestingly, the omVAT T_{reg} up-signature was significantly enriched and the corresponding down-signature significantly impoverished in the transcriptome of T_{regs} isolated from mice lacking PPAR γ only in T_{regs} (compared with their WT littermates) (Fig. 4A). These observations argue that obesity might exert its impact somewhere at the level of PPAR γ . However, in neither model did VAT T_{regs} from obese mice express fewer *Pparg* transcripts than their lean counterparts did (Fig. 4B). Hence, we were prompted to explore other known aspects of PPAR γ biology.

Spiegelman and colleagues recently discovered that many PPAR γ ligands exert anti-diabetic activities through a previously unsuspected biochemical pathway independent of classical PPAR γ agonism and its downstream transcriptional consequences (7–9). Diet-induced obesity activates cyclin-dependent kinase (Cdk5) and ERKs in adipocytes, leading to phosphorylation of the serine residue at position 273 (Ser273) of PPAR γ , which in turn results in dysregulation of a set of genes abnormally expressed in the obese state. Certain PPAR γ ligands, such as rosiglitazone and MRL24, are antidiabetic because they block Cdk5-induced phosphorylation of PPAR γ . These processes were detected in adipose tissue ex vivo, and could be mimicked in adipocyte cultures treated with tumor necrosis factor (TNF) α .

We hypothesized that analogous phosphorylation of PPAR γ at the Ser273 position might underlie at least some of the transcriptome changes induced in VAT T_{regs} by obesity. Unfortunately, by-far-inadequate cell numbers precluded testing this hypothesis on ex vivo T_{regs} by biochemical means. Instead, we made use of a TNF α -supplemented culture system parallel to that which had been used for adipocytes by Spiegelman and colleagues. Conventional Foxp3⁺CD4⁺ T cells were isolated from lean B6 mice, activated in vitro, and cotransduced with retroviruses expressing *Foxp3* and *Pparg*. We had previously demonstrated that the concomitant expression of these two genes in naïve CD4⁺ T_{conv} cells induced much of the VAT T_{reg} signature typical of lean mice (5). We first checked to what extent TNF α treatment of *Foxp3/Pparg*-transduced cells mimicked the T_{reg} transcriptome changes induced by obesity in vivo. As illustrated by a volcano plot comparing the effects of 24-h TNF α versus vehicle treatment, the omVAT T_{reg} up-signature was strongly induced by TNF α , whereas the corresponding down-signature was essentially unaltered (Fig. 5A). We then determined to what extent the TNF α -induced transcriptional changes reflected Ser273 phosphorylation. In the absence of TNF- α , the *Foxp3* transductants cotransduced with wild-type *Pparg* (*Pparg*-WT) and those transduced with *Pparg* encoding an Ala substitution for the Ser at position 273 (*Pparg*-S273A) showed indistinguishable expression of the omVAT T_{reg} up- and

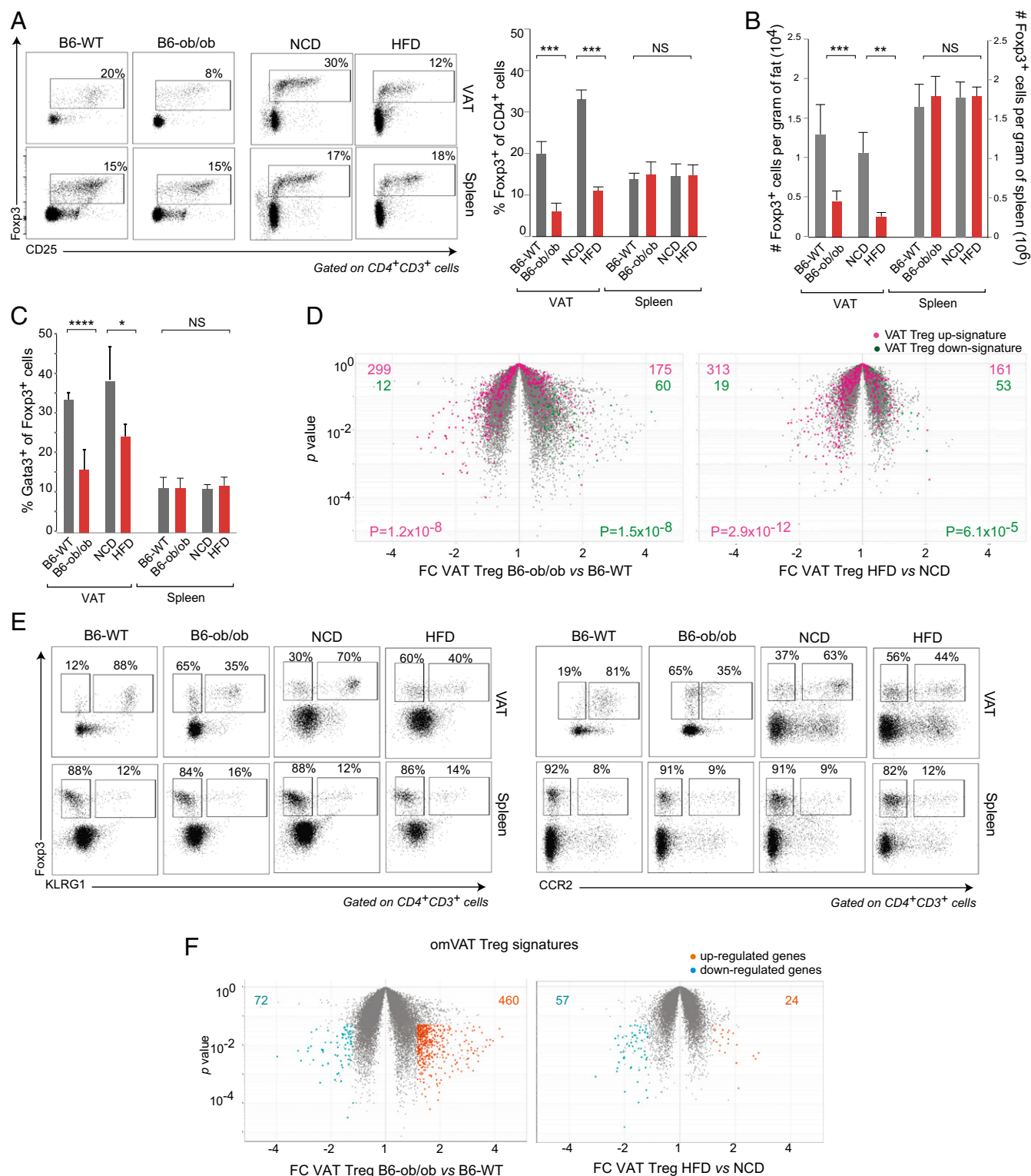


Fig. 3. T_{reg} numbers and phenotype in obese mice. (A–C) T_{reg} cell representation in the CD4⁺ compartment. Cells were isolated from the VAT and spleen of 14-wk-old B6-ob/ob vs. B6-WT mice or of B6 mice fed HFD vs. NCD between the ages of 8 and 16 wk. Percentage Foxp3⁺ of CD4⁺ T cells (A), number of such cells (B), and percentage Gata3⁺ of Foxp3⁺ cells were analyzed and displayed as per the corresponding panels in Fig. 1. For A–C, mean \pm SD; * P < 0.05; ** P < 0.01; *** P < 0.001; NS, not significant; by the Student's t test. (D) Volcano plots comparing transcriptomes of obese and lean mice in the two models. Overlain are the VAT T_{reg} up- (pink) and down- (green) signatures (from Dataset S1). P values from the χ^2 test. (E) Representative dot plots of Klrp1 (Left) and Ccr2 (Right) expression by VAT and spleen T_{regs} from obese mice and their lean controls. Percentages refer to the fraction of Foxp3⁺ cells constituted by the gated population. (F) Volcano plots comparing transcriptomes of obese and lean mice for the two models. Highlighted are the transcripts up- (orange) or down- (aqua) regulated ≥ 1.5 -fold in obese mice (with a P value of ≤ 0.05 in three replicates). The omVAT T_{reg} up- and down-signatures sum the altered transcripts from the two models (Dataset S2).

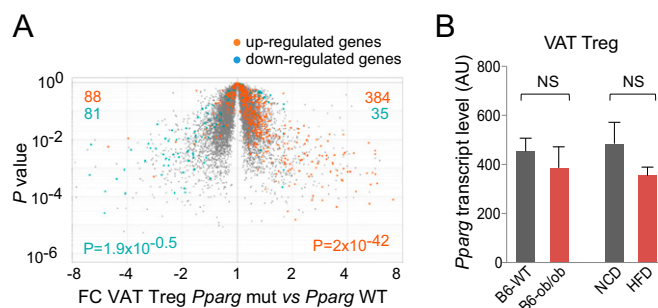


Fig. 4. PPAR γ and transcriptome changes with obesity. (A) Volcano plot comparing the VAT T_{reg} transcriptomes of mice lacking PPAR γ only in T_{reg}s (T_{reg} *Pparg* mut) vs. of their WT littermates (*Pparg* WT). Highlighted are the omVAT T_{reg} up- (orange) and down- (aqua) signatures (from Dataset S2). *P* values from the χ^2 test. (B) *Pparg* transcript levels. Extracted from the microarray data of Fig. 3. Mean \pm SD. NS = *P* value not significant by the Student's *t* test.

down-signatures (Fig. 5B); however, in the presence of TNF α , the up-signature was greatly enriched in the double-transductants expressing WT compared with the mutant PPAR γ (Fig. 5C). Furthermore, pretreatment of the *Foxp3*/*Pparg* double-transductants with SR1664, a Cdk5 inhibitor with no agonistic activity for PPAR γ (7), abolished the TNF α -induced differential between WT and mutant PPAR γ (Fig. 5D).

Western blotting with mAbs recognizing PPAR γ or specifically the phosphorylated Ser273 residue of PPAR γ confirmed the expected phosphorylation status of the *Foxp3*/*Pparg* double-transductants (Fig. 5E). TNF α induced phosphorylation at position 273 in WT, but not mutant, PPAR γ ; and TNF α -induced Ser273

phosphorylation was dampened by both the PPAR γ ligand, pio, and the Cdk5 inhibitor, SR1664.

Discussion

The transcriptome of VAT T_{reg}s is strikingly different from that of classical T_{reg}s circulating through lymphoid tissues (4, 5). Notably, transcripts encoding certain transcription factors (e.g., PPAR γ , Gata-3), chemokines or their receptors (e.g., CCR1, CCR2), cytokines or their receptors (e.g., IL10, IL1r1), and a set of proteins involved in lipid metabolism (e.g., Dgat1, Pcyt1a) are overrepresented in T_{reg}s residing in VAT. The overall goal of this study was to further elucidate the VAT T_{reg} signature: how it responds to aging in lean mice, to metabolic perturbation in obese mice, and to certain PPAR γ -mediated signaling events discovered in adipocytes.

Although the fraction of T_{reg}s in the VAT CD4⁺ T-cell compartment was routinely much higher than that in lymphoid organs in 25-wk-old mice, the differential was not apparent until about 10–15 wk of age, and 5-wk-old mice harbored a T_{reg} population in VAT fractionally similar to, or even smaller than, that in the spleen and LNs (ref. 4 and Fig. 1A and B). One possibility was that VAT is populated by T_{reg}s of lymphoid-type early in life, which are gradually replaced by their VAT-type counterparts, optimally adapted to thrive and proliferate. However, we found that the VAT T_{reg} signature was already evident at 5 wk of age. Paradigmatic VAT T_{reg} transcripts were already overrepresented, and for most of them there was little additional increase in expression at 25 wk: e.g., *Pparg* (1.3-fold), *Gata3* (1.4-fold), *Ccr2* (2.6-fold), *Klhl1* (1.7-fold), *Il1r1* (1.8-fold). There was, however, a score of transcripts enriched substantially more (>4 times) in the VAT T_{reg} population of 25- than of 5-wk-old mice; their continued increase might reflect additional local adaptation to the lipophilic, hypoxic adipose-tissue environment.

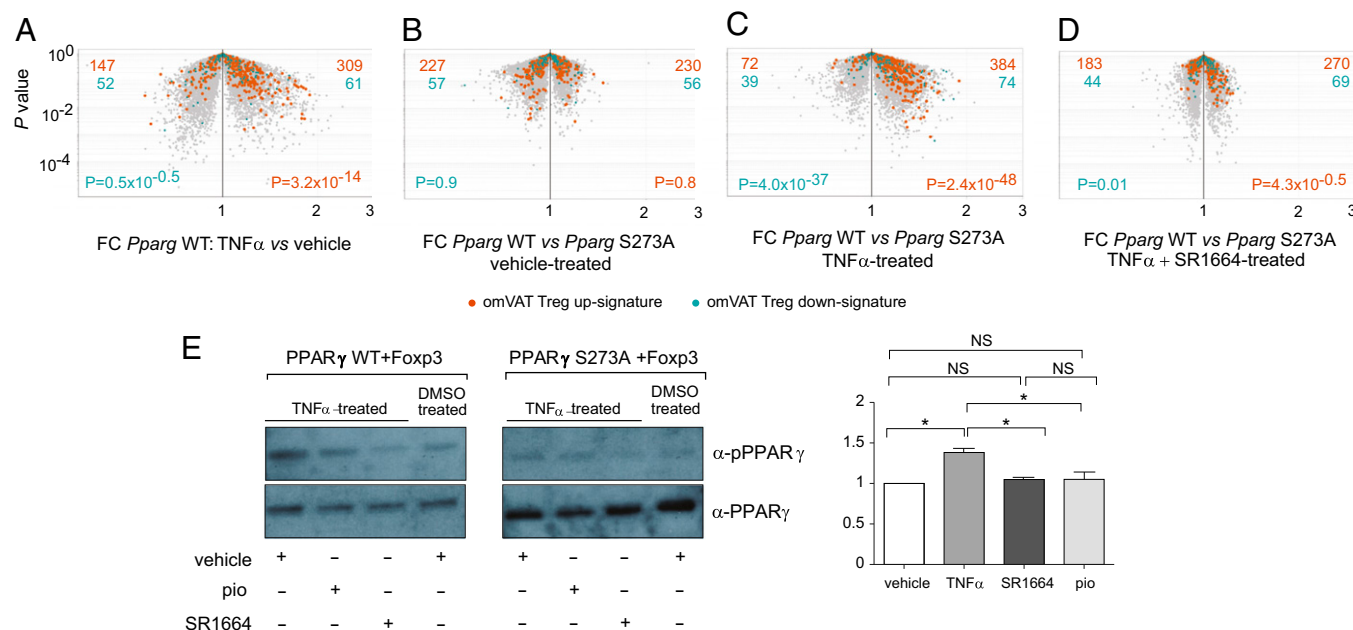


Fig. 5. Effect of PPAR γ phosphorylation on the VAT T_{reg} signatures. Naïve CD25⁺CD4⁺ T cells were stimulated ex vivo, and were transduced with retroviruses encoding *Foxp3* and WT *Pparg* (*Pparg* WT) or *Pparg* bearing the S273A phosphorylation-site mutation. Infected cells were treated with TNF α or vehicle in the presence or absence of the Cdk5 inhibitor, SR1664, and then were sorted for GFP and Thy1.1 positivity before RNA processing. (A–D) Microarray analysis. Volcano plots comparing the effects of TNF α (A), of the S273A mutation in the absence (B) or presence (C) of TNF α , and of the Cdk5 inhibitor, SR 1664, in the presence of TNF α (D). Highlighted are the omVAT T_{reg} up- (orange) and down- (aqua) signatures. *P* values from the χ^2 test. (E) Western blotting. Same samples as in A–D, except an additional sample from cells treated with TNF α plus pio was included. (Left) An example blot using Abs that detect total PPAR γ (clone E-8, Santa Cruz) or PPAR γ phosphorylated at position 273 (7). (Right) Quantification from two experiments. For each experiment, the value for vehicle-treated cells was set at 1. Mean \pm SD; **P* = <0.05; NS, not significant; by the Student's *t* test.

The first suggestion that VAT T_{regs} might have an important function in guarding against adipose-tissue inflammation and insulin resistance was their conspicuous reduction in insulin-resistant models of obesity, a notion ultimately substantiated by gain- and loss-of-function experiments (4, 5). In the present study, we showed this numerical decrease to be accompanied by loss of a large swathe of the VAT T_{reg} signature in the remaining Foxp3⁺CD4⁺ T-cell population, no matter whether obesity was provoked by a genetic or dietary alteration. Interestingly, about 1/3 of the VAT T_{reg} up-signature was not down-regulated in each of the two models.

In this study, we also defined an omVAT T_{reg} signature, consisting of transcripts up- or down-regulated in obese mice vis-à-vis their lean counterparts. Surprisingly, although this signature showed a strong correlation with transcriptional changes provoked by ablation of PPAR γ (Fig. 44), the level of transcripts encoding PPAR γ , itself, was not altered in the obese state. Instead, experiments on a previously and currently validated (ref. 8 and Fig. 54) TNF α -supplemented cell-culture model led us to conclude that PPAR γ must be phosphorylated at the Ser273 position by Cdk5. This posttranslational modification led to dysregulated transcription akin to what was previously reported for adipocytes (ref. 8 and Fig. 5).

These findings point to a remarkable parallelism in PPAR γ 's modus operandi in adipocytes and VAT T_{regs}. It is thus easier to rationalize our previous observation that the PPAR γ displayed on T_{regs} is a major conduit for the insulin-sensitizing effects of the PPAR γ agonists, such as pio and rosiglitazone, that were for many years front-line drugs for treatment of T2D (5). And one might anticipate that new PPAR γ agonists designed to have potency in the absence of weight gain, fluid retention, and cardiac abnormalities (7) will effectively target VAT T_{regs} as well as adipocytes. Lastly, this remarkable parallelism between the T_{reg} population and its parenchymal cohabitants highlights the malleability of T_{regs} in adapting to a particular tissue context, operating in concert with its defining cellular participant.

Methods

Mice. B6, B6.Lep^{ob/ob}, and B6.Pparg-flox (10) mice were bred in our specific-pathogen-free facilities at Harvard Medical School, or were purchased from Jackson Laboratory. T_{reg}-Pparg mut mice were generated as described (5). HFD-fed animals were maintained on a diet of 60 kcal% fat, purchased from Research Diets (catalog no. D12451). NCD-fed control animals were kept on a diet containing 10 kcal% fat, obtained from the same vendor (catalog no. 12450B). In designated experiments, pio (Actos, Takeda) was introduced into the diet at a concentration of 100 mg per kg of food. Experimental and control animals were generally littermate-matched males.

HOMA-IR, calculated as described (11), was determined for 25- and 40-wk-old B6 individuals. Mice were fasted overnight, weighed, then tested for fasting blood-glucose and blood-insulin concentrations by ELISA, performed by the Joslin Diabetes Center's Specialized Assay Core.

Immunocyte Isolation and Analysis. Epididymal adipose tissue (VAT) and splenic or LN immunocytes were isolated as described (4, 5). They were routinely stained with anti-CD45 (30-F11), -CD3 (145-2C11), -CD4 (GK1.5), -CD8 (5H10), and -CD25 (PC61) mAbs, (all eBiosciences) and, for some experiments, were fixed and permeabilized according to the manufacturer's instructions, followed by intracellular staining of Foxp3 (FJK-16s) and/or Gata3 (TWAJ) (both from eBiosciences). Cells were double-sorted using the MoFlo, or analyzed using an LSRII instrument (BD Bioscience) and FlowJo software.

Retroviral Transduction Experiments. Immunocytes were harvested from pooled spleens and LNs of 6- to 8-wk-old B6 mice, and CD25⁺CD4⁺ T cells were prepared for retroviral transduction as described (5). Viruses were made by transfecting platE cells (12) with (i) retroviral expression plasmids [MSCV IRES-GFP (pMIG2) and IRES-Thy1.1 (pMIT2)] (13), encoding Foxp3 (GFP), PPAR γ WT (Thy1.1) or PPAR γ S273A (Thy1.1); and (ii) the packaging construct pCL-ECO (14); using TransIT-293 (Mirus) according to the manufacturer's instructions. Naive CD4⁺ T cells were infected with retroviral supernatants 48 h after activation with anti-CD3/CD28 mAb-coated beads, and were cultured for an additional 72 h. Singly (Foxp3) or doubly (Foxp3 plus Pparg WT or Pparg S273A) transduced cells were double-sorted as (CD11b⁺CD11c⁺B220⁺CD8⁺CD3⁺CD4⁺GFP⁺(and/or Thy1.1⁺) by MoFlo for RNA processing and microarray analysis. In designated experiments, 48 h after cell infection, single- and double-transductants were treated with TNF α (50 ng/mL) with or without SR1664 (2 μ M) (7) or vehicle (DMSO) alone for 24 h.

Microarray Analysis. LN or VAT T_{regs} (CD25^{hi}CD4⁺CD3⁺) or T_{conv} cells (CD25⁺CD4⁺CD3⁺) were double-sorted from B6-WT, B6-ob/ob, Pparg WT or T_{reg}-Pparg mut mice. GFP⁺ (i.e., Foxp3⁺)CD4⁺CD3⁺ double-transduced cells, treated with TNF α plus SR1664 or vehicle, were also double-sorted to ensure high purity. RNA was extracted, amplified for two rounds, biotin-labeled, and purified as described (5). The resulting cRNAs (three independent datasets for each sample type) were hybridized to Mouse Genome M1.0 ST arrays (Affymetrix) according to the manufacturer's protocol. Microarray data were background-corrected and normalized, and replicates were averaged as described (5). The "VAT T_{reg}" signatures included transcripts \geq twofold over- or underrepresented in VAT T_{regs} vs. LN T_{regs}, VAT T_{conv} cells and LN T_{conv} cells of 25-wk-old mice. The omVAT T_{reg} signatures included all transcripts \geq 1.5-fold over- or underrepresented in VAT T_{regs} of obese mice vis-à-vis their lean comparators, summing those from the B6-ob/ob and HFD-fed models.

Immunoblotting. Foxp3⁺CD4⁺ T cells were cotransduced with Foxp3 and Pparg(WT or encoding the S273A mutant), pretreated with pio or SR1664 in DMSO or just DMSO, before incubation with DMSO or TNF α in DMSO. Protein lysates were made, run on SDS/PAGE, and probed with an anti-PPAR γ or an anti-phosphoPPAR γ (pPPAR γ) antibody, all as per ref. 7.

ACKNOWLEDGMENTS. We thank V. Babatunde for help with cloning, K. Hattori for assistance with mouse husbandry, J. LaVecchio and G. Buruzala for flow-cytometry, J. Ericson and K. Leatherbee for RNA processing, S. Davis for help with the microarray analysis, and Dr. M. T. Wilson for discussions. This work was supported by grants from the NIH (R01 DK092541), the Ellison Foundation (Boston), and the JPB Foundation (to D.M. and B.M.S.), and by the core facilities of the Joslin Diabetes Center (P30DK36836).

- Osborn O, Olefsky JM (2012) The cellular and signaling networks linking the immune system and metabolism in disease. *Nat Med* 18(3):363–374.
- Mathis D (2013) Immunological goings-on in visceral adipose tissue. *Cell Metab* 17(6):851–859.
- Cipolletta D (2014) Adipose tissue-resident regulatory T cells: Phenotypic specialization, functions and therapeutic potential. *Immunology* 142(4):517–525.
- Feuerer M, et al. (2009) Lean, but not obese, fat is enriched for a unique population of regulatory T cells that affect metabolic parameters. *Nat Med* 15(8):930–939.
- Cipolletta D, et al. (2012) PPAR- γ is a major driver of the accumulation and phenotype of adipose tissue Treg cells. *Nature* 486(7404):549–553.
- Tontonoz P, Spiegelman BM (2008) Fat and beyond: The diverse biology of PPAR- γ . *Annu Rev Biochem* 77:289–312.
- Choi JH, et al. (2011) Antidiabetic actions of a non-agonist PPAR γ ligand blocking Cdk5-mediated phosphorylation. *Nature* 477(7365):477–481.
- Choi JH, et al. (2010) Anti-diabetic drugs inhibit obesity-linked phosphorylation of PPAR γ by Cdk5. *Nature* 466(7305):451–456.

- Banks AS, et al. (2014) An ERK/Cdk5 axis controls the diabetogenic actions of PPAR γ . *Nature*, 10.1038/nature13887.
- Akiyama TE, et al. (2002) Conditional disruption of the peroxisome proliferator-activated receptor gamma gene in mice results in lowered expression of ABCA1, ABCG1, and apoE in macrophages and reduced cholesterol efflux. *Mol Cell Biol* 22(8):2607–2619.
- Matthews DR, et al. (1985) Homeostasis model assessment: Insulin resistance and beta-cell function from fasting plasma glucose and insulin concentrations in man. *Diabetologia* 28(7):412–419.
- Morita S, Kojima T, Kitamura T (2000) Plat-E: An efficient and stable system for transient packaging of retroviruses. *Gene Ther* 7(12):1063–1066.
- Holst J, et al. (2006) Generation of T-cell receptor retrogenic mice. *Nat Protoc* 1(1):406–417.
- Naviaux RK, Costanzi E, Haas M, Verma IM (1996) The pCL vector system: rapid production of helper-free, high-titer, recombinant retroviruses. *J Virol* 70(8):5701–5705.